SIAM J. NUMER. ANAL.
Vol. 57, No. 4, pp. 1770–1788

NUMERICAL METHOD FOR MULTI-ALLELES GENETIC DRIFT PROBLEM*

SHIXIN XU†, XINFU CHEN‡, CHUN LIU§, AND XINGYE YUE¶

Abstract. Genetic drift describes random fluctuations in the number of genes variants in a population. One of the most popular models is the Wright–Fisher model. The diffusion limit of this model is a degenerate diffusion-convection equation. Due to the degeneration and convection, Dirac singularities will always develop at the boundaries as time evolves, i.e., the fixation phenomenon occurs. Theoretical analysis has proven that the weak solution of this equation, regarded as measure, conserves total probability and expectations. In the current work, we propose a scheme for 3-alleles model with absolute stability and generalize it to N-alleles case ($N > 3$). Our method can conserve not only total probability and expectations, but also positivity. We also prove that the discrete solution converges to a measure as the mesh size tends to zero, which is the exact measure solution of the original problem. The simulations illustrate that the probability density decays to zero first on the inner nodes, then also on the edge nodes except at the three vertex nodes, on which the density finally concentrates. The results correctly predict the fixation probability and are consistent with theoretical ones and with direct Monte Carlo simulations.

Key words. multi-alleles genetic drift, degenerate diffusion-convection equation, measure solution, complete solution, fixation

AMS subject classifications. 65M06, 65N22, 92B05

DOI. 10.1137/18M1211581

1. Introduction.

Genetic drift is one of the mechanisms that cause changes over time in frequencies of an allele, which is an alternative form of a gene located at a specific position on a specific chromosome [14]. For example, there are different alleles which determine the gene for blood type in humans. In a finite population, the DNA coding of alleles determines distinct traits that can be passed from patents to offspring through sexual reproduction and the allele's frequency shifts by random chance. The simplest model of random genetic drift is known as the Wright–Fisher model by Wright [19, 20] and Fisher[7]. Moran [8] and Kimura [9, 12, 10, 11] derived the diffusion limit of random Wright–Fisher model. In this paper, we perform a mathematical and numerical analysis of the model.

The model derivation and numerical analysis for 2-alleles could be found in [21, 6, 22]. In this work we focus on the genetic drift problem about 3-alleles, denoted by A, B, and C, at a given locus in a population with a fixed size $\mathcal{N}$. Then, there are a total of $\bar{n} := 2\mathcal{N}$ alleles in the population of any generation. Under the assumptions of the Wright–Fisher model, the random process is a discrete-time Markov chain. Let $\mathbf{X}_k = (x_k, y_k)$, where x_k and y_k denote the fractions of alleles A and B, respectively,

*Received by the editors September 10, 2018; accepted for publication (in revised form) May 9, 2019; published electronically July 25, 2019.
https://doi.org/10.1137/18M1211581
Funding: The work of the authors was supported by the National Science Foundation grant DMS-1516344 and by the National Natural Science Foundation of China grants 11271281 and 91230106.

†School of Mathematical Sciences, Soochow University, Suzhou, Jiangsu, 215006, China, and Zu Chongzhi Center for Mathematics and Computational Sciences, Duke Kunshan University, No. 8 Duke Avenue, Kunshan, Jiangsu, 215316, China (xsxztr@hotmail.com).
‡Department of Mathematics, University of Pittsburgh, Pittsburgh, PA 15260 (xinfu@pitt.edu).
§Department of Applied Mathematics, Illinois Institute of Technology, Chicago, IL 60616 (cliu124@iit.edu).
¶School of Mathematical Sciences, Soochow University, Suzhou, 215006 Jiangsu, China (xyyue@suda.edu.cn).

in the kth generation. The transition probability is assumed to be

$$\mathbb{P}\Big(\mathbf{X}_{k+1} = (\tfrac{i}{\bar{n}}, \tfrac{j}{\bar{n}})\Big|\mathbf{X}_k = (x,y)\Big) = \frac{x^i y^j (1-x-y)^{\bar{n}-i-j}\ \bar{n}!}{i!j!(\bar{n}-i-j)!} \tag{1.1}$$

for each $i, j \in \{0, 1, \ldots, \bar{n}\}$ with $i + j \le \bar{n}$ and for each

$$(x,y) \in \big\{(\tfrac{i}{\bar{n}}, \tfrac{j}{\bar{n}}) \mid i, j \in \{0,1,\ldots,n\}, i+j \le \bar{n}\big\}.$$

Note that $z_k := 1 - x_k - y_k$ is the fraction of allele C in the kth generation. Using the transition probability, the first and second conditional moments could be given by

$$\mathbb{E}(\mathbf{X}_{k+1}|\mathbf{X}_k) = \mathbf{X}_k,$$
$$\mathrm{Cov}\left((\mathbf{X}_{k+1}, \mathbf{X}_{k+1})\Big|\mathbf{X}_k = (x,y)\right) = \frac{1}{\bar{n}}\begin{pmatrix} x - x^2 & -xy \\ -xy & y - y^2 \end{pmatrix}.$$

Thus, $\{\mathbf{X}_k\}_{k=0}^{\infty}$ is a martingale process, which is called neutral. Waxman [18] proved that for a neutral Wright–Fisher model without mutation, the phenomenon of *fixation* will happen; that is, after sufficient generations, only one of the alleles remains in the population. The fixation probability of each allele is equal to its initial fraction.

Given a population with a total of $\bar{n}$ alleles and a probability measure μ_0 of the initial distribution of $\boldsymbol{X}_0^{\bar{n}}$, the transition probability (1.1) determines a unique stochastic process $\{\boldsymbol{X}_k^{\bar{n}}\}_{k=0}^{\infty}$. We scale the time by setting $t_k = k/(2\bar{n})$ and $X_{t_k}^{\bar{n}} = \mathbf{X}_k^{\bar{n}}$. As $\bar{n} \to \infty$, $\{X_{t_k}^{\bar{n}}\}_{k=0}^{\infty}$ approaches a continuous stochastic Markov process $\{X(t)\}_{t\ge 0}$. Let $\mu(t)$ be the probability distribution of $X(t)$. It is regarded as a bounded functional over continuous functions by, for any $\zeta \in C^0(\bar{\Omega})$,

$$\langle \mu(t), \zeta\rangle = \int_\Omega \zeta(x,y)u(x,y,t)dxdy + \sum_{i=1}^{3}\left[\int_0^1 v_i(s,t)\zeta(\boldsymbol{x}_i(s)ds + \zeta(P_i)w_i(t)\right], \tag{1.2}$$

and subject to an initial state as a point measure

$$\mu_0 = \delta(x^0, y^0), \tag{1.3}$$

which means that the initial fractions of three alleles are, respectively, x^0, y^0, and $z^0 = 1 - x^0 - y^0$. Here we denote

$$\begin{gathered} \Omega = \{(x,y) \mid x > 0, y > 0, z := 1 - x - y > 0\}, \\ \boldsymbol{x}_1(s) = (0,s),\ \boldsymbol{x}_2(s) = (s,0),\ \boldsymbol{x}_3(s) = (s, 1-s), \\ \Gamma_i = \{\boldsymbol{x}_i(s) \mid s \in (0,1)\}, \qquad P_1 = (1,0),\ P_2 = (0,1),\ P_3 = (0,0). \end{gathered} \tag{1.4}$$

Thus, $u(\cdot,\cdot,t)$ is indeed the probability density of $X(t)$ on Ω, $v_i(\cdot,t)$ on Γ_i, and $w_i(t)$ on P_i. One can derive that $(u, v_1, v_2, v_3, w_1, w_2, w_3)$ is a solution of an initial value problem of the following partial and ordinary differential equations [17]:

$$\begin{cases} u_t(x,y,t) &= [(x-x^2)u]_{xx} + [(y-y^2)u]_{yy} - 2[xyu]_{xy}, \quad (x,y) \in \bar{\Omega}, \\ v_{i,t}(s,t) &= [(s-s^2)v_i]_{ss} + u(\boldsymbol{x}_i(s),t), \quad i = 1,2,3, \qquad s \in [0,1], \\ \begin{bmatrix} w_1(t) \\ w_2(t) \\ w_3(t) \end{bmatrix}_t &= \begin{bmatrix} v_2(1,t) + v_3(1,t) \\ v_1(1,t) + v_3(0,t) \\ v_1(0,t) + v_2(0,t) \end{bmatrix}, \qquad t > 0. \end{cases} \tag{1.5}$$

Here subscripts $[\cdot]_{xx}$, $[\cdot]_{xy}$, $[\cdot]_{yy}$, $[\cdot]_{ss}$ denote partial derivatives. The initial state shall be one of the following situations:

- the initial point measure centers inside the domain, i.e., $(x^0, y^0) \in \Omega$,

$$\begin{cases} u(x,y,0) = u^0(x,y) := \delta(x^0,y^0), \ (x,y) \in \Omega, \\ v_i(s,0) = v_i^0(s) := 0, \quad i = 1,2,3, \\ w_i(0) = w_i^0 := 0, \quad i = 1,2,3; \end{cases} \tag{1.6}$$

- the initial point measure centers at one of the edges, i.e., $(x^0, y^0) \in \Gamma_{i_0}$,

$$\begin{cases} u(x,y,0) = u^0(x,y) := 0, \ (x,y) \in \Omega, \\ v_{i_0}(s,0) = v_{i_0}^0(s) := \delta(s_0), \quad s_0 \in (0,1), i_0 \in \{1,2,3\}, \\ v_i(s,0) = v_i^0(s) := 0, \quad i \neq i_0 \in \{1,2,3\}, \\ w_i(0) = w_i^0 := 0, \quad i = 1,2,3; \end{cases} \tag{1.7}$$

- the initial point measure centers at one of the vertexes, i.e., $(x^0, y^0) = P_{i_0}$,

$$\begin{cases} u(x,y,0) = u^0(x,y) := 0, \ (x,y) \in \Omega, \\ v_i(s,0) = v_i^0(s) := 0, \quad i = 1,2,3, \\ w_{i_0}(0) = w_{i_0}^0 := 1, \quad i_0 \in \{1,2,3\}, \\ w_i(0) = w_i^0 := 0, \quad i \neq i_0 \in \{1,2,3\}. \end{cases} \tag{1.8}$$

The density function f of $\mu(t)$ can be expressed as

$$f = u + \sum_{i=1}^{3} v_i \delta_{\Gamma_i} + \sum_{i=1}^{3} w_i \delta_{P_i}. \tag{1.9}$$

Here δ_{Γ_i} is the line Dirac measure concentrated on the edge Γ_i and δ_{P_i} is the point Dirac measure concentrated on the vertex P_i, which are defined as $< \delta_{\Gamma_i}, \phi >= \int_{\Gamma_i} \phi ds$, and $< \delta_{P_i}, \phi >= \phi(P_i)$ for any $\phi \in C(\bar{\Omega})$. We call f in (1.9) a *complete* solution [21, 22] of the Wright–Fisher equation

$$f_t = \mathcal{L}f := [(x - x^2)f]_{xx} - 2[xyf]_{xy} + [(y - y^2)f]_{yy} \quad \text{on } \bar{\Omega} \times (0, \infty). \tag{1.10}$$

To illustrate that *fixation* probabilities $(v_1, v_2, v_3, w_1, w_2, w_3)$ are related by the above equation, we define the adjoint $\mathcal{L}^*$ of $\mathcal{L}$ under the L^2 inner product by

$$\mathcal{L}^*\zeta := (x - x^2)\zeta_{xx} - 2xy\zeta_{xy} + (y - y^2)\zeta_{yy}. \tag{1.11}$$

A complete solution of (1.10) in terms of measure is defined as follows.

DEFINITION 1.1. *Let a probability measure μ_0 on $\bar{\Omega}$ be given as in* (1.3). *A* complete *solution of* (1.10) *with initial measure μ_0 is a family of probability measures $\{\mu(t)\}$ on $\bar{\Omega}$ such that for any $T > 0$ and any $\zeta \in C^{2,1}(\bar{\Omega} \times [0,T])$,*

$$\Big\langle \mu(T), \zeta(\cdot, T) \Big\rangle - \int_0^T \Big\langle \mu(t), \zeta_t(\cdot,t) + \mathcal{L}^*\zeta(\cdot,t) \Big\rangle dt = \Big\langle \mu_0, \zeta(\cdot,0) \Big\rangle. \tag{1.12}$$

Here $C^{2,1}(\bar{\Omega} \times [0,T])$ consists of functions having continuous second order spatial derivatives and first order time derivative.

This definition of a complete solution is equivalent to that $\mu(t)$ is given by (1.2) with a family of functions $\{u, v_1, v_2, v_3, w_1, w_2, w_3\}$ satisfying (1.5) subject to one of the initial states (1.6)–(1.8).

Taking $\zeta = 1$, we obtain conservation of total probability. Taking $\zeta(x, y, t) = x$ and $\zeta(x, y, t) = y$, respectively, we obtain conservation of expectations

$$(\bar{x}, \bar{y}) := \mathbb{E}[X_t] = \mathbb{E}[X_0] = (x^0, y^0) \quad \forall\, t \geq 0. \tag{1.13}$$

Tran, Hofrichter, and Jost in [16] solved the eigenproblem for the operator $\mathcal{L}$ and $\mathcal{L}^*$, constructed a solution via Fourier series, and showed that the solution satisfies, with $\bar{z} := 1 - \bar{x} - \bar{y}$,

$$\lim_{t\to\infty} (u, v_1, v_2, v_3, w_1, w_2, w_3) = (0, 0, 0, 0, \bar{x}, \bar{y}, \bar{z}).$$

This illustrates the *fixation* phenomenon of the Wright–Fisher model.

This paper is devoted to the design of a numerical scheme that provides a complete solution. We intend to discretize (1.10) to obtain a complete solution given by (1.5). One main contribution of this paper is to extend the original state space $\bar{\Omega}$ to $\mathbb{R}^2$ and convert (1.10) to the following form:

$$f_t = \mathcal{L}f := \frac{\partial^2}{\partial x^2}\Big(x^+ z^+ f\Big) + \frac{\partial^2}{\partial y^2}\Big(y^+ z^+ f\Big) + \Big(\frac{\partial}{\partial x} - \frac{\partial}{\partial y}\Big)^2\Big(x^+ y^+ f\Big), \tag{1.14}$$

where $z = 1 - x - y$ and $a^+ = \max\{a, 0\}$. We notice that in the literature, "no-flux" boundary conditions with certain specific meaning were frequently imposed on the boundaries $\{x = 0\}, \{y = 0\}$, and $\{z = 0\}$. Here, we enlarge the state space to $\mathbb{R}^2$, which implies those "no-flux" boundary conditions. Please note that the no-flux boundary conditions are also implied in the definition of (1.12). Also, we extend the covariance matrix in such a way that the probability density is supported on the state space $\bar{\Omega}$ if initially so. We shall discretize (1.14) in a manner such that it is symmetric in x, y, and $z := 1 - x - y$ preserves the total probability, expectations, and the positivity. Note that problem (1.10) is degenerated and there exists a second order mixed derivative term. It is a considerably difficult task to discretize (1.10) in its original form to obtain a monotonic scheme which maintains positivity (see [13]).

For two-alleles problem, the corresponding governing equation is

$$f_t(x, t) = (x(1 - x)f)_{xx} = (x(1 - x)f_x)_x + ((1 - 2x)f)_x$$

for $x \in [0, 1]$ and $t > 0$. One could regard $-x(1-x)f_x$ as a diffusion flux and $-(1-2x)f$ as a convection flux. For the convection-dominated equation, the upwind scheme is typically a good choice. However, the authors in [21] proved that an upwind scheme will violate the conservation of expectations due to the numerical dissipation and proposed an absolute stable central difference scheme based on finite volume method.

The method in [21] cannot be extended directly to the 3-allele problem. Instead, based on the new formula (1.14), a numerical scheme is designed to find a *complete solution*. The scheme preserves the discrete total probability, expectations, and positivity. Some estimates on discrete L^∞ and H^1 norms are given to show the absolute stability of this scheme. Both the numerical analysis and simulations illustrate that the probability density decays to zero first on the inner nodes, then also on the edge nodes except at the three vertex nodes, on which the density finally concentrates. The results correctly predict the fixation probability and are consistent with theoretical ones and with direct Monte Carlo simulations. We also prove that the discrete solution converges to a measure, which is the exact solution of problems (1.10) and (1.3) as the mesh size tends to zero. It means that we prove again the existence of

the solution of the problem, which was first proved in [16] by a constructive method. Taking into account more factors such as selection or mutation [15], the method in [2, 16] may fail since one can hardly construct the solution; our discrete method will still work. This is another contribution of the paper. Furthermore, our method could be easily extended to the case of N-alleles ($N > 3$).

This paper is organized as follows. The numerical scheme, corresponding convergence, and stability analysis are presented in section 2. In section 3, simulations with different initial values are used to illustrate that the scheme could admit a complete solution and capture the fixation phenomenon of 3-alleles evolution. The conclusions and discussions are given in section 4.

2. Numerical analysis.

2.1. The numerical scheme. In this section, we present the discretization of the operator $\mathcal{L}$ in (1.14). In fact, $\mathcal{L}$ is indeed a surface diffusion operator on the equilateral triangle S defined by

$$S = \{(x, y, z) \mid x \geq 0, x \geq 0, z \geq 0, x + y + z = 1\}.$$

Also, $\mathcal{L}$ is symmetric in x, y, z. Thus, we first discretize the original physical space by equilateral triangle meshes and then project the equilateral triangle mesh of S onto $\bar{\Omega}$ to design the corresponding discretization of $\mathcal{L}$ on $\mathbb{R}^2$; see Figure 1.

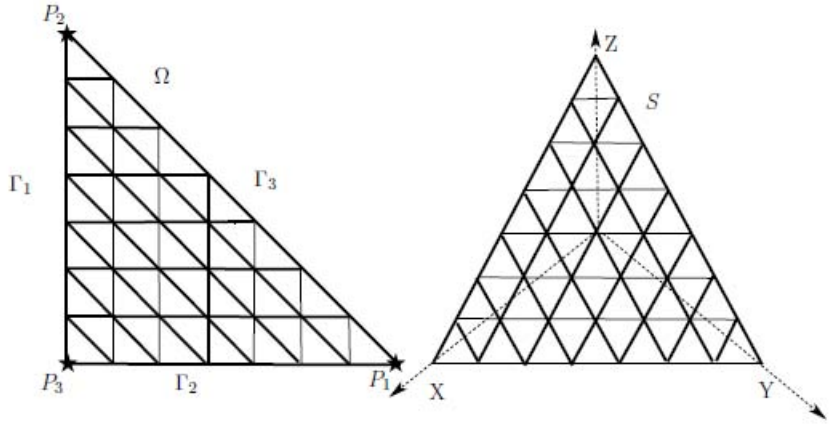

FIG. 1. *Schematic of computational domain.*

Let $h = 1/n, \Delta t = T/m$ for some positive integers n and m be the spatial and temporal mesh sizes, respectively. We use grid points

$$x_i = ih, \quad y_j = jh, \quad z_{ij} = 1 - x_i - y_j, \quad t_k = k\Delta t.$$

We discretize (1.10) as follows:

$$\frac{f_{ij}^k - f_{ij}^{k-1}}{\Delta t} = \sum_{d=1}^{3} D_d^2(\sigma_d f)_{ij}^k, \qquad i, j \in \mathbb{Z}, k \in \mathbb{N}, \tag{2.1}$$

where we use notation $\phi_{ij}^k = \phi_{i,j}^k = \phi(x_i, y_j, t_k)$ and D_1^2, D_2^2, and D_3^2 are second order finite differences along lines parallel to the x, y, and z level sets, respectively:

$$\begin{aligned}
&\sigma_1 = x^+ z^+, \quad D_1^2\phi_{ij}^k = \frac{1}{h^2}\Big\{\phi_{i+1,j}^k - 2\phi_{ij}^k + \phi_{i-1,j}^k\Big\},\\
&\sigma_2 = y^+ z^+, \quad D_2^2\phi_{ij}^k = \frac{1}{h^2}\Big\{\phi_{i,j+1}^k - 2\phi_{ij}^k + \phi_{i,j-1}^k\Big\},\\
&\sigma_3 = x^+ y^+, \quad D_3^2\phi_{ij}^k = \frac{1}{h^2}\Big\{\phi_{i+1,j-1}^k - 2\phi_{ij}^k + \phi_{i-1,j+1}^k\Big\}.
\end{aligned} \tag{2.2}$$

As to the initial values $\{f_{ij}^0 \mid (i,j) \in \mathbb{Z}^2\}$, we take the situation (1.6) $(x^0, y^0) \in \Omega$ as an example. Assume that $x^0 = i_0 h, y^0 = j_0 h$, then

$$f_{i_0,j_0}^0 = h^{-2}; \quad f_{ij}^0 = 0 \ \text{ if } (i,j) \neq (i_0, j_0) \in \mathbb{Z}^2. \tag{2.3}$$

Then we could obtain the initial total probability and expectations as follows:

$$\sum_{i,j=-\infty}^{\infty} f_{ij}^0\, h^2 = 1, \quad \sum_{i,j=-\infty}^{\infty} x_i f_{ij}^0\, h^2 = x^0 = \bar{x}, \quad \sum_{i,j=-\infty}^{\infty} y_j f_{ij}^0\, h^2 = y^0 = \bar{y}. \tag{2.4}$$

We divide the spatial index $(i,j) \in \mathbb{Z}^2$ into four groups:

1. *Exterior nodes*: $\bar{\Omega}_n^c := \{(i,j) \mid i < 0 \text{ or } j < 0 \text{ or } i + j > n\}$.
2. *Interior nodes*: $\Omega_n := \{(i,j) \in \mathbb{Z}^2 | 1 \le i, 1 \le j, i + j \le n - 1\}$.
3. *Interior edge nodes*: $\Gamma_n = \Gamma_n^1 \cup \Gamma_n^2 \cup \Gamma_n^3$, where

$$\Gamma_n^1 = \{(0,j) \mid 1 \le j \le n-1\}, \qquad \Gamma_n^2 = \{(i,0) \mid 1 \le i \le n-1\},$$
$$\Gamma_n^3 = \{(l, n-l) \mid 1 \le l \le n-1\}.$$

4. *Vertex nodes*: $P_n = P_n^1 \cup P_n^2 \cup P_n^3$,

$$P_n^1 = (n,0), \quad P_n^2 = (0,n), \quad P_n^3 = (0,0).$$

Then, we have the following well-posedness theorem of the numerical scheme (2.1)–(2.3).

THEOREM 2.1. *The scheme* (2.1)–(2.3) *admits a unique nonnegative solution*

$$\{f_{ij}^k | (i,j) \in \mathbb{Z}^2, k \in \mathbb{N}\}.$$

In addition, the following holds:

1. *For exterior nodes,* $f_{ij}^k = 0$ *each* $k \ge 1$ *and* $(i,j) \in \bar{\Omega}_n^c$.
2. *For interior nodes,* $\{f_{i,j}^k \mid (i,j) \in \Omega_n\}$ *form a closed system:*

$$\frac{f_{ij}^k - f_{ij}^{k-1}}{\Delta t} = D_1^2(xzf)_{ij}^k + D_2^2(yzf)_{ij}^k + D_3^2(xyf)_{ij}^k. \tag{2.5}$$

3. *For interior edge nodes, i.e., for* $i, j, l = 1, 2, \ldots, n-1$,

$$\begin{aligned}
&\frac{f_{i,0}^k - f_{i,0}^{k-1}}{\Delta t} = D_1^2(xzf)_{i,0}^k + \frac{z_{i,1} f_{i1}^k + x_{i-1} f_{i-1,1}^k}{h},\\
&\frac{f_{0,j}^k - f_{0,j}^{k-1}}{\Delta t} = D_2^2(yzf)_{0,j}^k + \frac{z_{1,j} f_{1j}^k + y_{j-1} f_{1,j-1}^k}{h},\\
&\frac{f_{l,n-l}^k - f_{l,n-l}^{k-1}}{\Delta t} = D_3^2(xyf)_{l,n-l}^k + \frac{x_{l-1} f_{l-1,n-l}^k + y_{n-l-1} f_{l,n-l-1}^k}{h}.
\end{aligned} \tag{2.6}$$

4. *For vertex nodes,*

$$\begin{aligned}\frac{f^k_{n,0}-f^{k-1}_{n,0}}{\Delta t}&=\frac{1-h}{h}\Big(f^k_{n-1,0}+f^k_{n-1,1}\Big),\\ \frac{f^k_{0,n}-f^{k-1}_{0,n}}{\Delta t}&=\frac{1-h}{h}\Big(f^k_{0,n-1}+f^k_{1,n-1}\Big),\\ \frac{f^k_{0,0}-f^{k-1}_{0,0}}{\Delta t}&=\frac{1-h}{h}\Big(f^k_{0,1}+f^k_{1,0}\Big).\end{aligned} \tag{2.7}$$

5. *For each $k\ge 1$, $\{f^k_{ij}\mid (i,j)\in\mathbb{Z}^2\}$ is a mean preserving probability measure in the sense that f^k_{ij} is nonnegative for any i,j and*

$$\sum_{i,j=-\infty}^{\infty} f^k_{ij}h^2=1,\quad \sum_{i,j=-\infty}^{\infty} x_i f^k_{ij}h^2=\bar{x},\quad \sum_{i,j=-\infty}^{\infty} y_j f^k_{ij}h^2=\bar{y}. \tag{2.8}$$

Proof. 1. When $i<0$ and $k=1$, (2.1) can be written as

$$f^1_{ij}=D_2^2(y^+z^+f)^1_{ij}\Delta t. \tag{2.9}$$

Thus, $f^1_{ij}=0$ when $j<0$ or $j>n-i$. When $0<j<n-i$, one has a closed system as $\mathbb{A}F=\vec{0}$ for $F=[f^1_{i1},f^1_{i2},\dots,f^1_{i,n-i-1}]^T$, since $yz=0$ at $j=0$ or $n-i$. Due to $-D_2^2(yz)_{ij}=-D_2^2(y(1-x_i-y))_j=2$, $\mathbb{A}$ is a tridiagonal M-matrix, i.e., diagonal entries are positive, off-diagonal entries are nonpositive, and the matrix is diagonal dominated. Thus, $F=\vec{0}$ is the only solution. Then from (2.9), $f^1_{ij}=0$ for $j=0$ or $n-i$. Hence, $f^1_{ij}=0$ if $i<0$. By induction, one can show that $f^k_{ij}=0$ for each $k\ge 1$ and $i<0$. After a similar analysis for the case $j<0$ and the case $i+j>n$, we conclude that $f^k_{ij}=0$ when $(i,j)\in\bar{\Omega}^c_{ij}$.

2. The interior node system (2.5) follows from (2.1). Note that the right-hand side of (2.5) depends only on the interior nodes, due to the fact that $xyz=0$ on the boundary of Ω. Thus, the system is closed, in a form as $\mathbb{B}F^k=F^{k-1}$, where F^k is a vector with all the unknowns $f^k_{i,j},(i,j)\in\Omega_n$, and $\mathbb{B}$ is a seven-diagonal matrix. Thanks to $-D_1^2(xz)=-D_2^2(yz)=-D_3^2(xy)=2$, B is a M-matrix. Then one has that the system admits a unique solution and the solution is nonnegative if F^{k-1} is nonnegative.

3. The interior edge systems (2.6) follow from (2.1). When the interior system (2.5) is solved, one has a closed system for interior edge unknowns at each edge. Each linear system has a tridiagonal M-matrix. So the solution is nonnegative since the interior unknowns have been shown to be nonnegative and unknowns at last time step are assumed to be nonnegative.

4. The assertion follows from (2.1) and the fact that $xyz=0$ on $\partial\Omega$.

5. The assertion follows by applying the following identity:

$$\sum_{ij}\phi_{ij}D_d^2(\sigma_d f)^k_{ij}=\sum_{ij}(\sigma_d f)^k_{ij}D_d^2\phi_{ij}$$

to linear functions. This completes the proof. ∎

As to the *numerical implementation*, for each time step $t_k,k=1,2,\dots$, one first solves the closed system (2.5) for interior unknowns $f^k_{ij},(i,j)\in\Omega_n$, then solves the three closed systems (2.6), respectively, for interior edge unknowns $f^k_{ij},(i,j)\in\Gamma_n$, and finally gets the unknowns at the three vertexes $f^k_{ij},(i,j)\in P_n$ from (2.7).

2.2. Convergence of the scheme and well-posedness of the PDE. We define

$$u_{ij}^k = f_{ij}^k \, \mathbf{1}_{\Omega_n}(\mathrm{i,j}), \quad v_{ij}^k = h f_{ij}^k \, \mathbf{1}_{\Gamma_n}(\mathrm{i,j}), \quad w_{ij}^k = h^2 f_{ij}^k \, \mathbf{1}_{P_n}(\mathrm{i,j}), \tag{2.10}$$

where $\mathbf{1}_A(a)$ is the indicate function: $\mathbf{1}_A(a) = 1$ if $a \in A$ and $\mathbf{1}_A(a) = 0$ otherwise. Let $\phi \in C_c^{2,1}(\mathbb{R}^2 \times [0,T])$ be a test function with compact support, and have continuous second order spatial derivatives and first order time derivative. Multiplying (2.1) by $-\phi_{ij}^k h^2 \Delta t$ and summing the resulting equation over i, j, and k, we obtain

$$\begin{aligned}
0 &= \sum_{k=1}^{m} \sum_{i,j=-\infty}^{\infty} h^2 \Big(\phi_{ij}^k (f_{ij}^{k-1} - f_{ij}^k) + \Delta t \phi_{ij}^k \sum_{d=1}^{3} D_d^2 (\sigma_d f)_{ij}^k \Big) \\
&= \sum_{i,j} \big(\phi_{ij}^1 f_{ij}^0 - \phi_{ij}^m f_{ij}^m \big) h^2 + \sum_{k=1}^{m-1} \sum_{i,j} f_{ij}^k \Big(\frac{\phi_{ij}^{k+1} - \phi_{ij}^k}{\Delta t} + \sum_{d=1}^{3} \sigma_d D_d^2 \phi_{ij}^k \Big) h^2 \Delta t \\
&= \sum_{(i,j)\in\Omega_n} \big(\phi_{ij}^1 u_{ij}^0 - \phi_{ij}^m u_{ij}^m \big) h^2 + \sum_{k=1}^{m-1} \sum_{(i,j)\in\Omega_n} u_{ij}^k \Big(\frac{\phi_{ij}^{k+1} - \phi_{ij}^k}{\Delta t} + \sum_{d=1}^{3} \sigma_d D_d^2 \phi_{ij}^k \Big) h^2 \Delta t \\
&+ \sum_{(i,j)\in\Gamma_n} \big(\phi_{ij}^1 v_{ij}^0 - \phi_{ij}^m v_{ij}^m \big) h + \sum_{k=1}^{m-1} \sum_{(i,j)\in\Gamma_n} v_{ij}^k \Big(\frac{\phi_{ij}^{k+1} - \phi_{ij}^k}{\Delta t} + \sum_{d=1}^{3} \sigma_d D_d^2 \phi_{ij}^k \Big) h \Delta t \\
&+ \sum_{(i,j)\in P_n} \big(\phi_{ij}^1 w_{ij}^0 - \phi_{ij}^m w_{ij}^m \big) + \sum_{k=1}^{m-1} \sum_{(i,j)\in P_n} w_{ij}^k \frac{\phi_{ij}^{k+1} - \phi_{ij}^k}{\Delta t} \, \Delta t.
\end{aligned} \tag{2.11}$$

We define $u^{h,\Delta t}(x,y,t), v_i^{h,\Delta t}(s,t), w_i^{h,\Delta t}(t)$, $i = 1,2,3$, as piecewise constant functions

$$\left\{ \begin{array}{rcll}
u^{h,\Delta t}(x,y,t) & = & u_{ij}^k, & (x,y,t) \in V_{ij} \times ((k-1)\Delta t, k\Delta t], \\
v_1^{h,\Delta t}(y,t) & = & v_{0,j}^k, & (y,t) \in (y_j - \frac{h}{2}, y_j + \frac{h}{2}] \times ((k-1)\Delta t, k\Delta t], \\
v_2^{h,\Delta t}(x,t) & = & v_{i,0}^k, & (x,t) \in (x_i - \frac{h}{2}, x_i + \frac{h}{2}] \times ((k-1)\Delta t, k\Delta t], \\
v_3^{h,\Delta t}(s,t) & = & v_{i,n-i}^k, & (s,t) \in (x_i - \frac{h}{2}, x_i + \frac{h}{2}] \times ((k-1)\Delta t, k\Delta t], \\
w_1^{h,\Delta t}(t) & = & w_{n,0}^k, & t \in ((k-1)\Delta t, k\Delta t], \\
w_2^{h,\Delta t}(t) & = & w_{0,n}^k, & t \in ((k-1)\Delta t, k\Delta t], \\
w_3^{h,\Delta t}(t) & = & w_{0,0}^k, & t \in ((k-1)\Delta t, k\Delta t],
\end{array} \right. \tag{2.12}$$

where $V_{ij} = (x_i - \frac{h}{2}, x_i + \frac{h}{2}] \times (y_j - \frac{h}{2}, y_j + \frac{h}{2}]$ is the control volume of node (x_i, y_j).

Denote $B_T := \bar{B} \times [0,T]$. For a temporal function $\psi \in C^0[0,T]$, we define its piecewise interpolation $I_T^{\Delta t}\psi$ in a backward way as in the definition (2.12). For a spatial function $\psi \in C^0(\bar{\Omega})$, we define its piecewise interpolations $I_B^h \psi$ in a central way as in the definition (2.12) with $B = \Omega$ or Γ_i, $i = 1,2,3$. For any $\psi \in C^0(\Omega_T)$, if we define its piecewise interpolations $I_{B_T}\psi = I_T^{\Delta t} \circ I_B^h \psi$ with $B = \Omega$ or Γ_i, then we have

$$\|\psi - I_{B_T}\psi\|_{L^\infty(B_T)} \to 0, \quad \text{as } h, \Delta t \to 0 \text{ for } B = \Omega, \Gamma_i, \text{ or } P_i. \tag{2.13}$$

For $\phi \in C^{2,1}(\Omega_T)$, if we denote by $\Box\phi = \phi_t + \mathcal{L}^*\phi$ and by $\Box^h \phi_{ij}^k = \frac{\phi_{ij}^{k+1} - \phi_{ij}^k}{\Delta t} + \sum_{d=1}^{3} \sigma_d D_d^2 \phi_{ij}^k$, we have

$$\max_{(i,j)\in\Omega_n, t_k \in [0,T]} |(\Box\phi)_{ij}^k - \Box^h \phi_{ij}^k| \longrightarrow 0, \text{ as } h, \Delta t \to 0. \tag{2.14}$$

With all of these notations, (2.11) can be rewritten as, for $\phi \in C^{2,1}(\Omega_T)$,

$$
\begin{aligned}
0 = \phi^1_{i_0,j_0} &- \int_\Omega u^{h,\Delta t}(x,y,T) I_\Omega \phi(x,y,T) dxdy + \int_0^{T'}\int_\Omega u^{h,\Delta t} I_{\Omega_T}(\Box\phi) dxdydt \\
&- \sum_{d=1}^{3}\left[\int_0^1 v_d^{h,\Delta t}(s,T) I_{\Gamma_d}\phi(\boldsymbol{x}(s),T)ds - \int_0^{T'}\int_0^1 v_d^{h,\Delta t}(s,t) I_{\Gamma_{d,T}}(\Box\phi)(\boldsymbol{x}(s),t)dsdt\right] \\
&- \sum_{d=1}^{3}\left[w_d^{h,\Delta t}(T)\phi(P_d,T) - \int_0^{T'} w_d^{h,\Delta t} I_T^{\Delta t}(\Box\phi)(P_d,t)dt\right] \\
&+ \sum_{k=1}^{m-1}\left[\sum_{(i,j)\in\Omega_n} u_{ij}^k\left(\Box\phi_{ij}^k - \Box^h\phi_{ij}^k\right)h^2\Delta t + \sum_{(i,j)\in\Gamma_n} v_{ij}^k\left(\Box\phi_{ij}^k - \Box^h\phi_{ij}^k\right)h\Delta t\right] \\
&+ \sum_{k=1}^{m-1}\sum_{(i,j)\in P_n} w_{ij}^k\left(\Box\phi_{ij}^k - \Box^h\phi_{ij}^k\right)\Delta t,
\end{aligned} \tag{2.15}
$$

where $T' = T - \Delta t$, and we have used $\Box\phi = \phi_t$ at the vertexes $P_i, i = 1,2,3$ and $v_{ij}^0 = w_{ij}^0 \equiv 0\ \forall(i,j)$. In order to take the limit in the above equation, we need the following *weak** compact result on Radon measures Proposition 1.48 in [5].

LEMMA 2.2. *Let $\{u_n\}$ be a nonnegative bounded sequence in $L^1(B)$. Then, $\{u_n\}$ is weakly* compact in $M(B)$, i.e., there exists a subsequence u_{n_k} and $u \in M(B)$ such that*

$$
\lim_{k\to\infty}\int_B u_{n_k}\phi dx = \langle u,\phi\rangle_{M(B),C_c^0(B)} \quad \textit{for any } \phi \in C_c^0(B), \tag{2.16}
$$

where $M(B) \subset (C_c^0(B))'$ is the set of nonnegative linear functional on $C_c^0(B)$, i.e., Radon measures.

Then, by Lemma 2.2 and the first equality of (2.8), we have, for any fixed $T > 0$ and up to a subsequence, that, when $h, \Delta t \longrightarrow 0$,

$$
\begin{aligned}
&u^{h,\Delta t} \longrightarrow u \in M(\Omega_T) \text{ weakly* in } M(\Omega_T), \\
&u^{h,\Delta t}(x,y,T) \longrightarrow \tilde{u}(x,y,T) \in M(\Omega) \text{ weakly* in } M(\Omega), \\
&v_i^{h,\Delta t} \longrightarrow v_i \in M(\Gamma_{i,T}) \text{ weakly* in } M(\Gamma_{i,T}),\ i = 1,2,3, \\
&v_i^{h,\Delta t}(s,T) \longrightarrow \tilde{v}_i(s,T) \in M(\Gamma_i) \text{ weakly* in } M(\Gamma_i),\ i = 1,2,3, \\
&w_i^{h,\Delta t} \longrightarrow w_i \in M([0,T]) \text{ weakly* in } M([0,T]),\ i = 1,2,3, \\
&w_i^{h,\Delta t}(T) \longrightarrow \tilde{w}_i(T),\ i = 1,2,3,
\end{aligned} \tag{2.17}
$$

where, to get the first five results, we set $B = \Omega_T, \Omega, \Gamma_{i,T}, \Gamma_i$, and $[0,T]$, respectively in Lemma 2.2.

Taking the limit of (2.15) along the subsequences and thanks to the inequalities

(2.13) and (2.14), we find that, for any $\phi \in C^{2,1}(\Omega_T)$,

$$
\begin{aligned}
0 =& \langle \delta(x^0, y^0), \phi(x, y, 0)\rangle - \int_\Omega \tilde{u}(x, y, T)\phi(x, y, T)dxdy + \int_0^T \int_\Omega u(x, y, t)[\phi_t + \mathcal{L}^*\phi]dxdydt \\
&- \sum_{d=1}^{3} \left[\int_0^1 \tilde{v}_d(s, T)\phi(\boldsymbol{x}_d(s), T)ds - \int_0^T \int_0^1 v_d(s, t)\Big(\phi_t + \mathcal{L}^*\phi\Big)(\boldsymbol{x}_d(s), t)dsdt \right] \\
&- \sum_{d=1}^{3} \left[\tilde{w}_d(T)\phi(P_d, T) - \int_0^T w_d(t)\phi_t(P_d, t)dt \right].
\end{aligned} \tag{2.18}
$$

Thanks to the above equation, we have $u(x, y, T) = \tilde{u}(x, y, T)$, $v_i(s, T) = \tilde{v}_i(s, T)$, and $w_i(T) = \tilde{w}_i(T)$, just as the initial condition is fulfilled $u(x, y, 0) = \delta(x^0, y^0)$ in the weak sense. This means $u^{h,\Delta t}(x, y, T) \longrightarrow u(x, y, T)$ weakly* in $M(\Omega)$, $v_i^{h,\Delta t}(s, T) \longrightarrow v_i(s, T)$ weakly* in $M(\Gamma_i)$, and $w_i^{h,\Delta t}(T) \longrightarrow w_i(T)$ in (2.17).

Thus, $(u, v_1, v_2, v_3, w_1, w_2, w_3)$ is a weak solution of (1.5)–(1.6), i.e., a complete solution of (1.10) and (1.3).

It was proved in [16] that there exists a unique distribution solution of the problem (1.10) and (1.3). The uniqueness leads to the fact that the sequences $u^{h,\Delta t}$, $v_i^{h,\Delta t}$, and $w_i^{h,\Delta t}$, $i = 1, 2, 3$ converge as a whole.

THEOREM 2.3. *The piecewise numerical solutions* (2.12) *from the discrete scheme* (2.1) *and* (2.3) *converge as the step size* $h, \Delta t \to 0$. *And the limit is a solution of the problem* (1.5) *and* (1.6).

2.3. Stability analysis of numerical scheme. In this section, we study the L^∞ and discrete H^1 stability of the numerical scheme, and long-time behavior of the numerical solution. The L^∞ estimates illustrate that the numerical solution at the inner nodes and edge nodes exponentially decays to zero and all the mass (or probability) is gradually concentrated to the three vertexes.

2.3.1. L^∞ stability and long-time behavior. If we define

$$
\begin{aligned}
M(t_k) &= \max_{(i,j)\in\Omega_n} f_{ij}^k, \\
M_1(t_k) &= \max_{(i,j)\in\Gamma_n} f_{ij}^k h, \\
M_2(t_k) &= \max\{\bar{x} - f_{n0}^k h^2, \bar{y} - f_{0n}^k h^2, \bar{z} - f_{00}^k h^2\},
\end{aligned}
$$

we have the following L^∞ stability results.

THEOREM 2.4. *For each* $t \in \{t_k\}_{k=0}^\infty$,

$$
M(t) \le M(0)e^{-6t\frac{\ln(1+6\Delta t)}{6\Delta t}}, \tag{2.19}
$$

$$
M_1(t) \le \Big[M_1(0) + \tfrac{1}{4}M(0)\Big]e^{-2t\frac{\ln(1+2\Delta t)}{2\Delta t}}, \tag{2.20}
$$

$$
M_2(t) \le \Big[M_1(0) + \tfrac{1}{4}M(0)\Big]e^{-2t\frac{\ln(1+2\Delta t)}{2\Delta t}}. \tag{2.21}
$$

Proof. Fix $k \ge 1$. Suppose $(i, j) \in \Omega_n$ is an interior node such that $f_{ij}^k = M(t_k)$. Then we obtain from (2.5) that

$$
\frac{M(t_k) - f_{ij}^{k-1}}{\Delta t} \le M(t_k)\Big\{D_1^2(xz)_{ij} + D_2^2(yz)_{ij} + D_3^2(xy)_{ij}\Big\} = -6M(t_k).
$$

Thus,

$$M(t_k) \le \frac{M(t_{k-1})}{1+6\Delta t} \le \cdots \le \frac{M(0)}{(1+6\Delta t)^k} = M(0)e^{-6t_k \frac{\ln(1+6\Delta t)}{6\Delta t}}.$$

Suppose $(i,j) \in \Gamma_n$ is an interior edge node such that $M_1(t_k) = f_{ij}^k h$. By symmetry, without loss of generality we can assume that $i = 0$. Then multiplying (2.6) by h we find that

$$\begin{aligned}\frac{M_1(t_k) - h f_{0j}^{k-1}}{\Delta t} &\le M_1(t_k) D_2^2 (yz)_{0j} + (z_{1j} + y_{j-1}) M(t_k) \\ &= -2M_1(t_k) + [1-2h]M(t_k).\end{aligned}$$

Thus,

$$\begin{aligned}M_1(t_k) &\le \frac{M_1(t_{k-1})}{1+2\Delta t} + \frac{\Delta t[1-2h]M(t_k)}{1+2\Delta t} \\ &\le \frac{M_1(t_{k-1})}{1+2\Delta t} + \frac{\Delta t\,[1-2h]M(0)}{(1+2\Delta t)(1+6\Delta t)^k}.\end{aligned}$$

By induction we obtain

$$\begin{aligned}M_1(t_k) &\le \frac{M_1(0)}{(1+2\Delta t)^k} + \sum_{m=0}^{k-1} \Big(\frac{1+2\Delta t}{1+6\Delta t}\Big)^{k-m} \frac{(1-2h)\Delta t}{(1+2\Delta t)^{k+1}} M(0) \\ &= \frac{M_1(0)}{(1+2\Delta t)^k} + \frac{1 - (\frac{1+2\Delta t}{1+6\Delta t})^k}{(1+2\Delta t)^k}\ \frac{(1-2h)M(0)}{4}.\end{aligned}$$

From (2.8) and the above uniform decay estimates we find that

$$\lim_{k\to\infty} f_{n0}^k h^2 = \bar{x}, \quad \lim_{k\to\infty} f_{0n}^k h^2 = \bar{y}, \quad \lim_{k\to\infty} f_{00}^k h^2 = \bar{z}.$$

In addition, from (2.7) we find that

$$0 \le \frac{f_{n0}^k h^2 - f_{n0}^{k-1} h^2}{\Delta t} \le 2(1-h)M_1(t_k) \le \frac{2[M_1(0) + \frac{1}{4}M(0)]}{(1+2\Delta t)^k.}.$$

Thus

$$\begin{aligned}0 \le \bar{x} - f_{n0}^k h^2 &= \sum_{m=k+1}^{\infty} [f_{n0}^m h^2 - f_{n0}^{m-1} h^2] \\ &\le 2\Delta t \Big[M_1(0) + \frac{1}{4}M(0)\Big] \sum_{m=k+1}^{\infty} \frac{1}{(1+2\Delta t)^m} \\ &= \frac{M_1(0) + \frac{1}{4}M(0)}{(1+2\Delta t)^k}.\end{aligned}$$

A similar estimate for f_{n0}^k and f_{00}^k then completes the proof of Theorem 2.4.

2.3.2. H^1 estimates. Now we consider the discrete H^1 stability of the numerical scheme. We introduce

$$D_1^+\phi_{ij}=\frac{\phi_{i+1,j}-\phi_{ij}}{h},\quad D_1^-\phi_{ij}=\frac{\phi_{ij}-\phi_{i-1,j}}{h},$$
$$D_2^+\phi_{ij}=\frac{\phi_{i,j+1}-\phi_{ij}}{h},\quad D_2^-\phi_{ij}=\frac{\phi_{ij}-\phi_{i,j-1}}{h},$$
$$D_3^+\phi_{ij}=\frac{\phi_{i+1,j-1}-\phi_{i,j}}{h},\quad D_3^-\phi_{ij}=\frac{\phi_{ij}-\phi_{i-1,j+1}}{h}.$$

Interior estimates. Since $u_{ij}^k=0$ when $(i,j)\notin\Omega_n$, we have

$$\sum_{i,j=-\infty}^{\infty}\frac{|u_{ij}^k-u_{ij}^{k-1}|^2+|u_{ij}^k|^2-|u_{ij}^{k-1}|^2}{\Delta t}=2\sum_{i,j}u_{ij}^k\frac{(u_{ij}^k-u_{ij}^{k-1})}{\Delta t}$$
$$=2\sum_{ij}u_{ij}^k\Big[D_1^2(xzu)_{ij}^k+D_2^2(yzu)_{ij}^k+D_3^2(xyu)_{ij}^k\Big]$$
$$=-\sum_{ij}\sum_{d=1}^{3}\sigma_{dij}\Big(\big|D_d^+u_{ij}^k\big|^2+\big|D_d^-u_{ij}^k\big|^2\Big)-6\sum_{ij}|u_{ij}^k|^2.$$

Multiplying both sides by $\Delta t(1+6\Delta t)^{k-1}$, ignoring the nonnegative term involving $|u_{ij}^k-u_{ij}^{k-1}|^2$, and summing over k, we then obtain the following estimate.

PROPOSITION 2.5. *If we let $u_{ij}^k=f_{ij}^k$ when $(i,j)\in\Omega_n$ and $u_{ij}^k=0$ otherwise, then*

$$\sum_{k=1}^{\infty}[1+6\Delta t]^{k-1}\Delta t\sum_{ij}\sum_{d=1}^{3}\sigma_{dij}\Big[\big|D_d^+u_{ij}^k\big|^2+\big|D_d^-u_{ij}^k\big|^2\Big]h^2\le\sum_{(i,j)\in\Omega_n}|f_{ij}^0|^2h^2,$$
$$\sup_{k\ge0}\ e^{6t_k\frac{\ln(1+6\Delta t)}{6\Delta t}}\sum_{i,j}|u_{ij}^k|^2h^2\le\sum_{(i,j)\in\Omega_n}|f_{ij}^0|^2h^2.$$

Boundary estimates. Next, we consider $v_i^k=v_{i0}^k$. Since $v_i^k=0$ when $(i,0)\notin\Gamma_n^2$, we have

$$2\sum_{i=-\infty}^{\infty}\frac{v_i^k(v_i^k-v_i^{k-1})}{\Delta t}=\sum_i v_i^k\Big(D_1^2(xzv)_{i0}^k+z_{i1}u_{i1}^k+x_{i-1}u_{i-1,1}^k\Big)$$
$$=-\sum_i x_i[1-x_i]\Big(\Big|\frac{v_{i+1}^k-v_i^k}{h}\Big|^2+\Big|\frac{v_i^k-v_{i-1}^k}{h}\Big|^2\Big)$$
$$-2\sum_i|v_i^k|^2+\sum_i(z_{i1}v_i^k+x_iv_{i+1}^k)u_{i,1}^k.$$

Thus, by Cauchy's inequality $ab\le(a^2+b^2)/2$, we obtain

$$\sum_i\frac{(1+\Delta t)|v_i^k|^2-|v_i^{k-1}|^2}{\Delta t}+\sum_i x_i(1-x_i)\Big(\Big|\frac{v_{i+1}^k-v_i^k}{h}\Big|^2+\Big|\frac{v_i^k-v_{i-1}^k}{h}\Big|^2\Big)$$
$$\le\sum_i\frac{(|z_{i1}|^2+|x_i|^2)|u_{i1}^k|^2}{2}\le\sum_{i=1}^{n-1}\frac{|u_{i1}^k|^2}{2}\le\frac{|M(t_k)|^2}{2h}\le\frac{|M(0)|^2}{2h[1+12\Delta t]^k}.$$

Hence, multiplying both sides by $(1+\Delta t)^{k-1}h\Delta t$ and summing over k, we obtain the following proposition.

PROPOSITION 2.6. *If we let* $v_i^k = hf_{i0}^k$ *for* $i = 1, \ldots, n-1$ *and* $v_i^k = 0$ *otherwise, then*

$$\sum_{k=1}^{\infty}(1+\Delta t)^{k-1}\Delta t\sum_{i=1}^{n-1} x_i(1-x_i)\left[\left|\frac{v_{i+1}^k - v_i^k}{h}\right|^2 + \left|\frac{v_i^k - v_{i-1}^k}{h}\right|^2\right]h \le \sum_{i=1}^{n-1} h|v_i^0|^2 + \frac{|M(0)|^2}{22}.$$

Discrete time derivative estimate. More particularly, if we set

$$g_{ij}^k = \frac{f_{ij}^{k+1} - f_{ij}^k}{\Delta t},$$

then, by linearity, $\{g_{ij}^k\}$ satisfies the same linear system as that of f:

$$\begin{aligned} \frac{g_{ij}^k - g_{ij}^{k-1}}{\Delta t} &= D_1^2(xzg)_{ij}^k + D_2^2(yzg)_{ij}^k + D_3^2(xyg)_{ij}^k, \\ g_{ij}^0 &= D_1^2(xzf^0)_{ij} + D_2^2(yzf^0)_{ij} + D_3^2(xyf^0)_{ij}. \end{aligned} \tag{2.22}$$

Same as the above proposition, we obtain the following estimate for $\{g_{ij}^k\}$.

PROPOSITION 2.7. *If we let* g_{ij}^0 *be defined as in* (2.22) *and set*

$$M_3(0) = \max_{(i,j)\in\Omega_n} |g_{ij}^0|, \qquad M_4(0) = \max_{(i,j)\in\Gamma_n} h|g_{ij}^0|,$$

then for each $k \ge 0$,

$$\sup_{(i,j)\in\Omega_n}\left|\frac{u_{ij}^{k+1} - u_{ij}^k}{\Delta t}\right| \le \frac{M_3(0)}{(1+6\Delta t)^k},$$

$$\sup_{(i,j)\in\Gamma_n}\left|\frac{v_{ij}^{k+1} - v_{ij}^k}{\Delta t}\right| \le \frac{M_4(0) + \frac{1}{4}M_3(0)}{(1+2\Delta t)^k}.$$

3. Simulation results. In this section, we present several simulation results by using the scheme (2.1)–(2.3). The results illustrate that the scheme is stable, positivity-preserving, and could yield a complete solution. The results correctly predict the *fixation* probability and are consistent with both theoretical results and direct Monte Carlo simulations.

Example 1. In this example, we test the consistency between 3-alleles and 2-alleles by choosing the fraction of allele C be zero in the two-dimensional (2D) model. The initial value is chosen as $\mu_0 = \delta(0.7, 0.3)$, and correspondingly

$$f_{ij}^0 = \begin{cases} h^{-2} & \text{if } (x_i, y_j) = (0.7, 0.3), \\ 0 & \text{otherwise,} \end{cases} \tag{3.1}$$

which means $(\bar{x}, \bar{y}, \bar{z}) = (0.7, 0.3, 0)$. The mesh size is chosen to be $h = 1/200$ and the time step is fixed as $\Delta t = 1/1000$. In this case, the 2D genetic problem is reduced to the one-dimensional (1D) problem. Figure 2 shows the simulation results with this initial value, which is not zero only on the boundary $z = 0$. Panels (a-d) confirm that values of inner nodes are always zero and evolution only happens on the boundary $z = 0$. The dynamics of values on the boundary $z = 0$ shown in Figure 3 is consistent with the results presented in [21] for the 1D genetic drift problem.

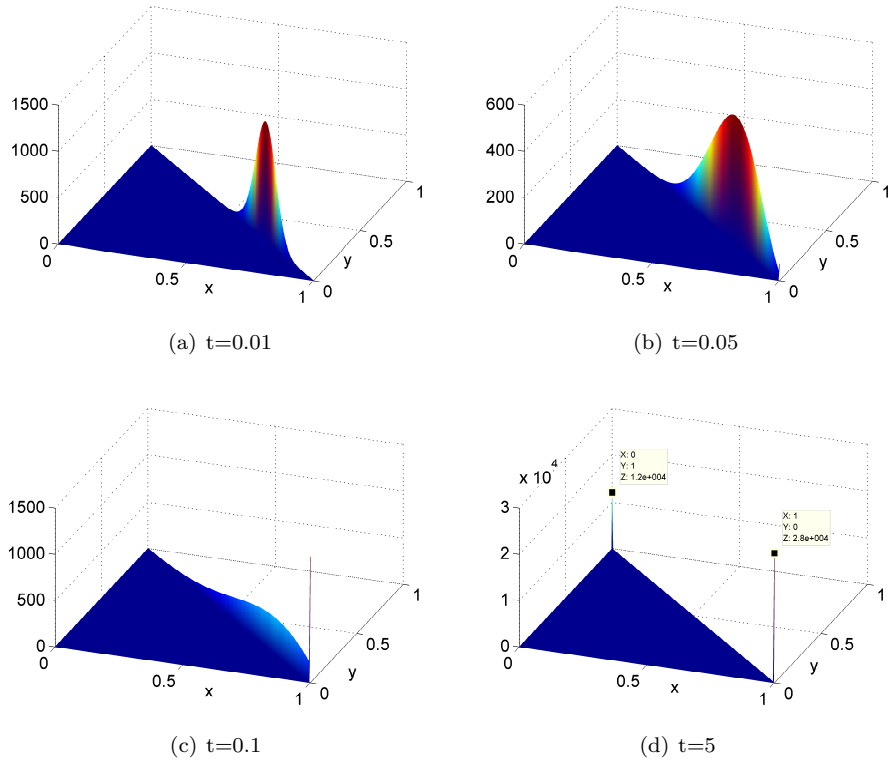

(a) t=0.01 (b) t=0.05

(c) t=0.1 (d) t=5

FIG. 2. *Numerical results with initial state* $(\bar{x}, \bar{y}, \bar{z}) = (0.7, 0.3, 0)$ *at different time* $t = 0.01, 0.05, 0.1, 5$. *The step sizes are* $h = 1/200, \Delta t = 1/1000$.

Example 2. In this example, we test two initial values with Dirac measures centered inside the domain Ω to show the evolutions of total probabilities inside the domain, on the edges and at vertex nodes, respectively.

We consider

$$f_{ij}^0 = \begin{cases} h^{-2} & \text{if } (x_i, y_j) = (0.4, 0.3), \\ 0 & \text{otherwise}, \end{cases} \tag{3.2}$$

which means $(\bar{x}, \bar{y}, \bar{z}) = (0.4, 0.3, 0.3)$. Next, we consider

$$f_{ij}^0 = \begin{cases} h^{-2} & \text{if } (x_i, y_j) = (0.3, 0.6), \\ 0 & \text{otherwise}, \end{cases} \tag{3.3}$$

which means $(\bar{x}, \bar{y}, \bar{z}) = (0.3, 0.6, 0.1)$.

In Figure 4, we plot the dynamics of genetic shift of alleles by the following functions:

$$m(t_k) = \sum_{(i,j)\in\Omega_n} f_{ij}^k h^2,$$

$$p_d(t_k) = \sum_{(i,j)\in\Gamma_n^d} f_{ij}^k h^2, \quad d = 1, 2, 3,$$

$$q_d(t) = \sum_{(i,j)\in P_n^d} f_{ij}^k h^2, \quad d = 1, 2, 3.$$

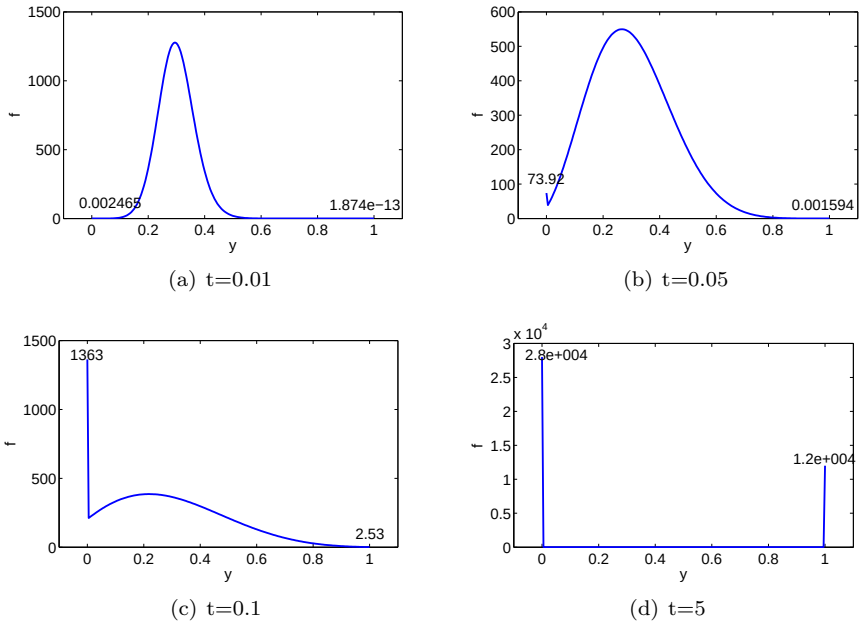

(a) t=0.01 (b) t=0.05

(c) t=0.1 (d) t=5

FIG. 3. *One-dimensional numerical results with initial state* f^0 *at different time* $t = 0.01, 0.05, 0.1, 5$ *at* $z = 0$. *The step sizes are* $h = 1/200, \Delta t = 1/1000$.

The curves $p_1(t), p_1(t) + p_2(t)$, $p_1(t) + p_2(t) + p_3(t)$, $p_1(t) + p_2(t) + p_3(t) + q_1(t)$, $p_1(t) + p_2(t) + p_3(t) + q_1(t) + q_2(t)$, $p_1(t) + p_2(t) + p_3(t) + q_1(t) + q_2(t) + q_3(t)$, and $1 = p_1(t) + p_2(t) + p_3(t) + q_1(t) + q_2(t) + q_3(t) + m(t)$ are plotted on the same picture to show the probabilities of mono allele and binary alleles populations. The left panel is the results for the initial value $(\bar{x}, \bar{y}, \bar{z}) = (0.4, 0.3, 0.3)$ and right panel is the results for the initial value $(\bar{x}, \bar{y}, \bar{z}) = (0.3, 0.6, 0.1)$. The simulation results for the initial value $(\bar{x}, \bar{y}, \bar{z}) = (0.4, 0.3, 0.3)$ are presented in Figure 5. Panels (a–d) illustrate that the probability density on the inner nodes first decay to zero, then the nodes on the edges decay to zero, and finally all of the mass are concentrated on three vertex nodes, which is consistent with our theoretical results.

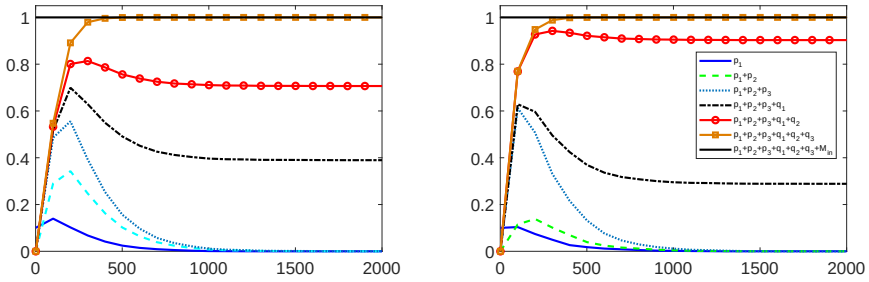

FIG. 4. *Dynamics of genetic shift of alleles. Left:* $(\bar{x}, \bar{y}, \bar{z}) = (0.4, 0.3, 0.3)$. *Right:* $(\bar{x}, \bar{y}, \bar{z}) = (0.3, 0.6, 0.1)$. *The step sizes are* $h = 1/200, \Delta t = 1/400$.

.

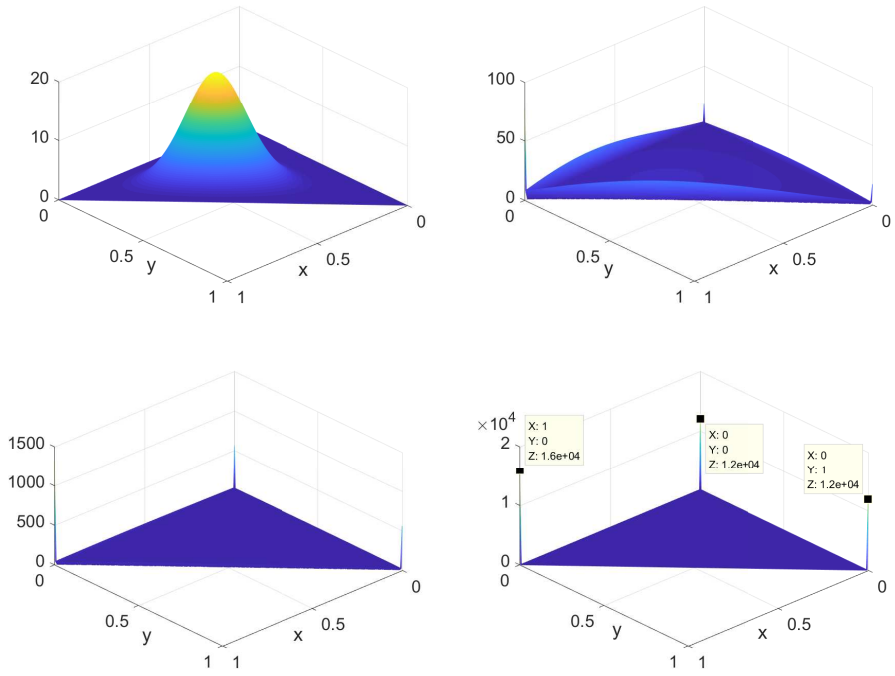

FIG. 5. *Numerical results with initial state* $(\bar{x}, \bar{y}, \bar{z}) = (0.4, 0.3, 0.3)$ *at different time* $t = 0.025, 0.125, 0.25, 12.5$. *The step sizes are* $h = 1/200, \Delta t = 1/400$. .

Example 3. In this example, we make a comparison between the direct Monte Carlo simulations for stochastic process (1.1) and numerical simulations for the PDE model (1.10). The initial states are the same as in Example 2. In Figure 6, the dynamics of mass on points (P_n^1, P_n^2 and P_n^3), edges (Γ_n^1, Γ_n^2 and Γ_n^3), and inner domain Ω_n of (1.10) are presented. Monte Carlo simulations are done with $\bar{n} = 2\mathcal{N} = 200$ alleles, 2000 time steps, and 5000 sample paths. PDE simulation results are obtained with mesh size $h = 1/(2\mathcal{N}), \triangle t = 1/(4\mathcal{N})$. These simulations demonstrate that both methods are consistent with each other.

4. Conclusions and discussions. We have proposed a numerical method for a 3-alleles genetic drift problem, which is a two-dimensional degenerate convection-dominated parabolic equation. Due to the degeneration, there will always be Dirac singularities developed at the boundary points $(0,0)$, $(1,0)$, and $(0,1)$. By introducing a variable $z = 1 - x - y$ and a directional derivative $\frac{\partial}{\partial \zeta} = \frac{\partial}{\partial x} - \frac{\partial}{\partial y}$, the scheme is designed to be symmetric to variables x, y, z. The numerical scheme is proved to be a stable scheme and could yield a *complete* solution, which preserves total probability, expectations, and positivity. The numerical simulations with different initial values illustrated the robustness of the scheme.

The method could be generated to N-alleles, $N > 3$ case. For example, the 4-alleles genetic problem could be described by following [16],

$$\partial_t f - \sum_{i,j=1}^{3} \partial_{ij}^2 \big((x_i \delta_{ij} - x_i x_j) f\big) = 0 \quad \text{on} \quad \bar{\Omega} \times (0, \infty), \tag{4.1}$$

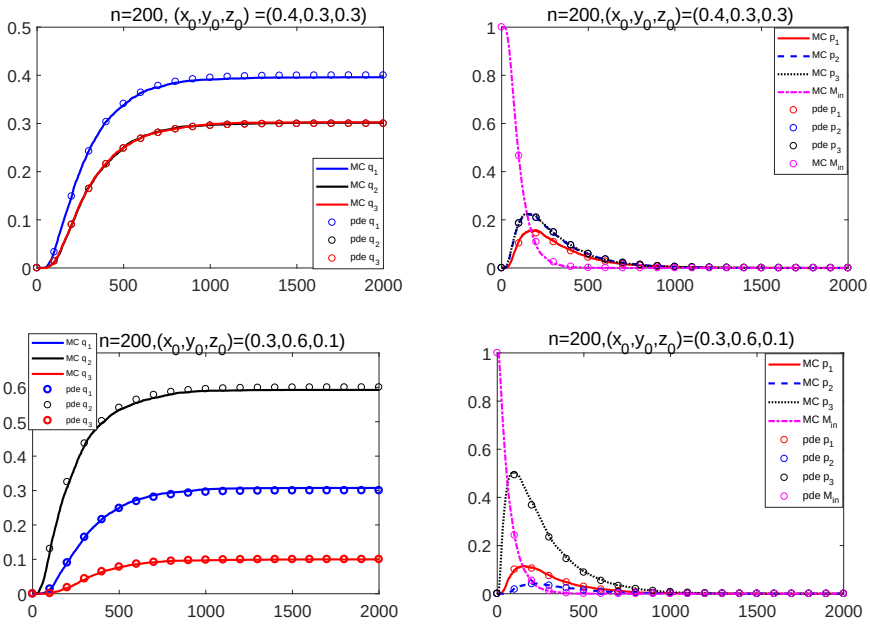

FIG. 6. *Comparison between Monte Carlo and PDE simulations. Top:* $(\bar{x}, \bar{y}, \bar{z}) = (0.4, 0.3, 0.3)$. *Bottom:* $(\bar{x}, \bar{y}, \bar{z}) = (0.3, 0.6, 0.1)$. *Left: Dynamics of mass at points* P_n^1, P_n^2, P_n^3. *Right: Dynamics of mass at edges* Γ_n^1, Γ_n^2, Γ_n^3 *and inner domain* Ω_n. *Lines: Monte Carlo simulation results. Circles: PDE simulation results. The step sizes are* $h = 1/200, \Delta t = 1/400$.

where $\delta_{ij} = 1$, for $i = j$, $\delta_{ij} = 0$, for $i \neq j$, $\Omega = \{(x_1, x_2, x_3) \mid x_1 > 0, x_2 > 0, x_3 > 0, x_4 \equiv 1 - x_1 - x_2 - x_3 > 0\}$, and x_1, x_2, x_3, x_4 are the fractions of the four alleles, respectively.

Similarly, due to the degeneration of the diffusion coefficient, the static solution has Dirac singularities at boundary points $(0,0,0)$, $(1,0,0)$, $(0,1,0)$, and $(0,0,1)$, i.e., one can observe the fixation phenomena. In order to design a stable scheme which could yield the *complete* solution, we rewrite the original equation into a more symmetric form:

$$\begin{aligned} \partial_t f = {} & \partial_{11}^2(x_1 x_4 f) + \partial_{22}^2(x_2 x_4 f) + \partial_{33}^2(x_3 x_4 f) \\ & + (\partial_1 - \partial_2)^2(x_1 x_2 f) + (\partial_2 - \partial_3)^2(x_2 x_3 f) + (\partial_3 - \partial_1)^2(x_3 x_1 f). \end{aligned} \tag{4.2}$$

In this new formula, a key feature is that we have six second order directional derivatives, just along side the six edges of the simplex Ω. We can approximate each of them by a second order 3-*points* central difference scheme. For example, on an equidistance mesh,

$$\begin{aligned} (\partial_1 - \partial_2)^2 u|_{i,j,k} &= \frac{u_{i+1,j-1,k} + u_{i-1,j+1,k} - 2u_{i,j,k}}{h^2} + O(h^2), \\ (\partial_2 - \partial_3)^2 u|_{i,j,k} &= \frac{u_{i,j+1,k-1} + u_{i,j-1,k+1} - 2u_{i,j,k}}{h^2} + O(h^2), \\ (\partial_3 - \partial_1)^2 u|_{i,j,k} &= \frac{u_{i+1,j,k-1} + u_{i-1,j,k+1} - 2u_{i,j,k}}{h^2} + O(h^2). \end{aligned}$$

Then similar results can be obtained as for 3-alleles in section 2. Of course, to prove the similar convergence as in Theorem 2.3, we have four scales now: keep the scale

inside the domain, rescale by h on the four sides, rescale by h^2 on the six edges, and rescale by h^3 at the four vertexes. For even more alleles problems $N > 4$, the method still works. However, it is not a practical numerical scheme any more due to the curse of dimension. Anyway, it could be used as a theoretical tool to prove the existence of solution to the original problem by compactness argument.

In Theorem 2.3, it is proved that the numerical solution weakly* converges to the exact solution as a measure on $\Omega \times (0, T)$, i.e., the whole domain with space and time. It is possible that the exact solution $f(x, t)$ in (1.9) is a probability measure in space and continuous in time. To verify this, one need at least prove an enhanced result that the numerical solution in (2.12) weakly* converges to $f(\cdot, t)$ in $M(\Omega)$ $\forall t \in [0, T]$. Similar results on measure solutions can be found in [1, 3, 4]. We will address this in future work.

In this paper we have only considered the simplest genetic drift case, where the only evolutionary force acting on a randomly mating diploid population is diffusion. The mutation, migration, and selection forces can be taken into account to generate analogous schemes. We will also discuss this in further work.

Acknowledgments. The authors benefited a great deal from discussions with Prof. Xiaobing Feng and Prof. David Waxman. The authors thank the anonymous referees for their most valuable comments which improved the paper.

REFERENCES

[1] L. Ambrosio, N. Gigli, and G. Savare, *Gradient Flows in Metric Spaces and in the Space of Probability Measures*, Lectures Math. ETH Zurich, Birkhauser Verlag, Basel, 2005.

[2] R. Burger, *The Mathematical Theory of Selection, Recombination, and Mutation*, John Wiley & Sons, Chichester, UK, 2000.

[3] J. A. Carrillo, M. Difrancesco, A. Figalli, T. Laurent, and D. Slepcev, *Global-in-time weak measure solutions and finite-time aggregation for nonlocal interaction equations*, Duke Math. J., 156 (2011), pp. 229–271.

[4] J. A. Carrillo, F. James, F. Lagoutiere, and N. Vauchelet, *The Filippov characteristic flow for the aggregation equation with mildly singular potentials*, J. Differential Equations, 260 (2016), pp. 304–338.

[5] D. Cioranescu and P. Donato, *An Introduction to Homogenization*, Oxford Lecture Ser. Math. Appl. 17, Oxford University Press, New York, 1999.

[6] C. Duan, C. Liu, C. Wang, and X. Yue, *Numerical complete solution for random genetic drift by Energetic Variational approach*, ESAIM Math. Model. Numer. Anal., 53 (2019), pp. 615–634.

[7] R. A. Fisher, *On the dominance ratio*, Proc. Roy. Soc. Edinburgh, 42 (1922), pp. 321–431.

[8] P. A. P. Moran, *Random processes in genetics*, Proc. Cambridge Philos. Soc., 54 (1958), pp. 60–72.

[9] M. Kimura, *Stochastic processes and distribution of gene frequencies under natural selection*, Cold Spring Harb. Symp. Quant. Biol., 20 (1955), pp. 33–53.

[10] M. Kimura, *Random genetic drift in multi-allelic locus*, Evolution, 9 (1955), pp. 419–435.

[11] M. Kimura, *On the probability of fixation of mutant genes in a population*, Genetics, 47 (1962), pp. 713–719.

[12] M. Kimura, *Diffusion models in population genetics*, J. Appl. Probability, 1 (1964), pp. 177–232.

[13] J. M. Nordbotten, I. Aavatsmark, and G. T. Eigestad, *Monotonicity of control volume methods*, Numer. Math., 106 (2007), pp. 255–288.

[14] L. C. Parish, S. Brenner, J. L. Parish, and M. Ramos-e-Silva, *Manual of Gender Dermatology*, Jones & Bartlett Publishers, Sudbury, MA, 2010.

[15] T. D. Tran, J. Hofrichter, and J. Jost, *The free energy method for the Fokker-Planck equation of the Wright-Fisher model*, Theory Boisci., 134 (2015), pp. 83–92, https://doi.org/10.1007/s12064-015-0218-2.

[16] T. D. Tran, J. Hofrichter, and J. Jost, *A general solution of the Wright-Fisher model of random genetic drift*, Differ. Equ. Dyn. Syst., (2016), pp. 1–26, https://doi.org/10.1007/s12591-016-0289-7.
[17] C. Tier and J. B. Keller, *A tri-allelic diffusion model with selection*, SIAM Appl. Math., 35 (1978), pp. 521–535, https://doi.org/10.1137/0135044.
[18] D. Waxman, *Fixation at a locus with multiple alleles: structure and solution of the Wright Fisher model*, J. Theoret. Biol., 257 (2009), pp. 245–251.
[19] S. Wright, *The evolution of dominance*, Amer. Nat., 63 (1929), pp. 556–561.
[20] S. Wright, *The differential equation of the distribution of gene frequencies*, Proc. Natl. Acad. Sci. USA, 31 (1945), pp. 382–389.
[21] S. Xu, M. Chen, C. Liu, R. Zhang, and X. Yue, *Behavior of different numerical schemes for random genetic drift*, BIT, accepted, https://doi.org/10.1007/s10543-019-00749-4.
[22] L. Zhao, X. Yue, and D. Waxman, *Complete numerical solution of the diffusion equation of random genetic drift*, Genetics, 194 (2013), pp. 973–985.